Excited-State Proton Transfer to Methanol–Water Mixtures

Noam Agmon,*

Department of Physical Chemistry and The Fritz Haber Research Center, The Hebrew University of Jerusalem, Jerusalem 91904, Israel

Dan Huppert, Asnat Masad,

School of Chemistry, Raymond and Beverly Sackler Faculty of Exact Sciences, Tel Aviv University, Tel Aviv 69978, Israel

and Ehud Pines

Department of Chemistry, The University of Chicago, 5735 South Ellis Avenue, Chicago, Illinois 60637
(Received: April 2, 1991)

We have measured the fluorescence decay of 8-hydroxypyrene-1,3,6-trisulfonate due to proton transfer to solvent in water–methanol mixtures. The data agree quantitatively with the reversible, diffusion-influenced proton-transfer mechanism in all solutions. No significant deviations from a short-time exponential decay or a long-time power law decay were found that could support a recently suggested water molecule diffusion mechanism. Solvent-induced variations in the deprotonation rate coefficient are very close to those in the corresponding equilibrium coefficient. Analysis of measured and literature pK data indicates that the composition dependence is mainly due to localized counterion stability in water-rich solutions and to proton stability in methanol-rich solutions. Quantitative agreement with literature compilations of proton-transfer free energy is obtained. These observations challenge the prevailing idea that a minimal cluster of four water molecules is the required proton acceptor in these solutions.

Introduction

Solvent effects on proton transfer to solvent raise important problems concerning the physical chemistry of solvation.[1] Particularly intriguing is the question of whether the solvent, which is also the proton acceptor, behaves as a continuous medium or are its molecular characteristics indispensable in understanding proton-transfer and proton solvation dynamics. Early conductivity measurements[2] have shown that the abnormal proton conductivity of pure water drastically diminishes in mixtures of methanol–water when the alcohol content is increased. The effect has been interpreted[1,2] as arising from water structure breaking by the organic cosolvent. It was thus concluded that the abnormally high proton conductivity in neat water is due to cooperative pairing of water molecules.

Picosecond lasers have enabled the study of proton (and electron) transfer to solvent from excited dye molecules.[3-13] Transient fluorescence decay from excited hydroxyaryls showed[3] that proton dissociation rates decrease sharply with increasing alcohol content of water–alcohol solutions. This decrease was apparently not explainable by the decrease of the solvent (static) dielectric constant, ϵ.[3] It has therefore been interpreted as further evidence for the destabilization of the proton-accepting complex namely, large water molecule clusters, with increasing alcohol content. A theory developed by Lee, Robinson, and collaborators[4-6] assumes that proton will only transfer to a solvent cluster containing a sufficient number of water molecules. The rate of proton transfer to solvent depends on the probability of having at least four water molecules in the hypothetical solvation shell of the would-be proton solvation site. Exchange of one or more of the four water molecules with alcohol molecules is considered as drastically depressing the proton-transfer reaction.

More recently, the Dhahran group[7] has extended our time-resolved investigations[9-13] of excited-state proton transfer from 8-hydroxypyrene-1,3,6-trisulfonate (HPTS) to water–methanol mixtures. They have suggested that the rate-determining step in proton transfer to such mixtures is the diffusion of a water molecule to the excited dye molecule.[7] This prepares the appropriate proton solvation site and allows proton dissociation. If this interpretation were correct, our reversible diffusive proton dissociation/recombination mechanism[9-13] would be a secondary effect, at best.

Our work has focused on the transient fluorescence decay, which starts as an exponential, turning over to a power law ($t^{-3/2}$) at long times. This we interpreted as evidence for the diffusive motion of the proton, which can rebind reversibly to the excited-state anion (without quenching it to the ground state), thus regenerating the excited-state acid. Our experimental work has triggered the development of the theory of *reversible* diffusion-influenced reactions,[14] as an extension of the theory of (irreversible) diffusion-limited reactions.[15] So far we have found quantitative agreement between theory and experiment.[10-13] The suggestion of the Dhahran group[7] implies that the long-time power law decay becomes unimportant (if it is there at all[7]) in mixtures of methanol–water, while it is the short-time behavior which should show

(1) Conway, B. E. In *Modern Aspects of Electrochemistry*; Bockris, J. O'M., Conway, B. E., Eds.; Butterworths: London, 1964; Vol. 3, Chapter 2.
(2) Conway, B. E.; Bockris, J. O'M.; Linton, H. *J. Chem. Phys.* **1956**, *24*, 834.
(3) Huppert, D.; Kolodney, E. *Chem. Phys.* **1981**, *63*, 401.
(4) (a) Moore, R. A.; Lee, J.; Robinson, G. W. *J. Phys. Chem.* **1985**, *89*, 3648. (b) Robinson, G. W.; Thistlethwaite, P. J.; Lee, J. *J. Phys. Chem.* **1986**, *90*, 4224.
(5) Lee, J.; Griffin, R. D.; Robinson, G. W. *J. Chem. Phys.* **1985**, *82*, 4920. Lee, J.; Robinson, G. W.; Webb, S. P.; Philips, L. A.; Clark, J. H. *J. Am. Chem. Soc.* **1986**, *108*, 6538.
(6) Lee, J. *J. Am. Chem. Soc.* **1989**, *111*, 427.
(7) Suwaiyan, A.; Al-Adel, F.; Hamdan, A.; Klein, U. K. A. *J. Phys. Chem.* **1990**, *94*, 7423.
(8) Masad, A.; Huppert, D. *Chem. Phys. Lett.* **1991**, *180*, 409.
(9) Pines, E.; Huppert, D. *Chem. Phys. Lett.* **1986**, *126*, 88. Pines, E.; Huppert, D. *J. Chem. Phys.* **1986**, *84*, 3576.
(10) (a) Pines, E.; Huppert, D.; Agmon, N. *J. Chem. Phys.* **1988**, *88*, 5620. (b) Agmon, N.; Pines, E.; Huppert, D. *J. Chem. Phys.* **1988**, *88*, 5631. (c) Huppert, D.; Pines, E.; Agmon, N. *J. Opt. Soc. Am. B* **1990**, *7*, 1545.
(11) (a) Pines, E.; Huppert, D. *J. Am. Chem. Soc.* **1989**, *111*, 4096. (b) Pines, E.; Huppert, D.; Agmon, N. In *Ultrafast Phenomena VI*; Springer Series in Chemical Physics 48; Springer Verlag: Berlin, 1988; p 517. (c) *J. Phys. Chem.* **1991**, *95*, 666.
(12) Agmon, N. *J. Chem. Phys.* **1988**, *88*, 5639; **1988**, *89*, 1524.
(13) Pines, E. Ph.D. Thesis, Tel-Aviv University, Tel-Aviv, 1989.
(14) Agmon, N.; Szabo, A. *J. Chem. Phys.* **1990**, *92*, 5270.
(15) Rice, S. A. Diffusion Limited Reactions. In *Comprehensive Chemical Kinetics*; Bamford, C. H., Tipper, C. F. H., Compton, R. G., Eds.; Elsevier: Amsterdam, 1985; Vol. 25.

0022-3654/91/2095-10407$02.50/0

a deviation from exponential decay. Indeed, competition of water molecules over binding to the acidic proton makes the dissociation step equivalent to fluorescence quenching, where several quenchers compete for trapping of the excitation. The problem can therefore be treated by the Smoluchowski approximation[16] namely, the protonated species decays as $\exp(-\alpha t - \beta t^{1/2})$, with α and β constants.

One of the goals of the present work is to perform an accurate measurement of HPTS fluorescence decay in methanol–water mixtures and check whether the theory of diffusion-influenced reactions still applies or else water diffusion becomes rate limiting, as suggested by the Dhahran group. Of equal importance is the critical evaluation of the conceptual basis for their suggestion of water molecule diffusion, namely, the water cluster model[4-6] for proton dissociation.

An argument often raised[3,4b] in support of the idea that the controlling factor is the extra proton stability in large water clusters is the findings from mass spectrometric gas-phase cluster data. These measurements show that the binding energy of an additional solvent molecule to gas-phase protonated clusters decreases as a function of cluster size and levels off at a cluster size of about 10. While this may indicate the participation of many solvent molecules in proton solvation, it does not mean that these must all be water molecules. In fact, recent gas-phase measurements[17] in mixed water–methanol clusters show that the proton affinity of methanol is considerably larger (by approximately 60 kJ/mol) than that of water and that preferential binding to methanol decreases yet persists in gas-phase clusters up to seven solvent molecules.

Analytical chemists have used solubility data together with some extrathermodynamic assumptions to obtain the free energy of transfer, ΔG_t, of a proton from water to various solutions.[18,19] While ions such as Cl^- behave in methanol–water mixtures qualitatively as suggested by the Born charging model, namely, they are destabilized (their ΔG_t values increase) with decreasing ϵ (i.e., increasing methanol content), H^+ shows a peculiar pattern.[18] Proton free energy is affected very little (less than 1 kJ/mol) by methanol content up to 80% (by weight). It is hard to see how such small variations can lead to orders of magnitude decrease in the proton dissociation rate.

Our excited-state proton-transfer system shows a large geminate recombination effect. Using single photon counting to monitor the long-time tails allows us therefore to determine not only the dissociation but also the recombination rate parameter at the contact distance. Hence, if we find that our data in methanol–water mixtures conform to the reversible diffusion theory, we could test whether the rate parameters obtained agree with the free energy of transfer data[18,19] or with the water cluster assumption.[4-7] This will provide important clues as to whether the molecularity of the solvent is manifested in the kinetic data in the simple manner suggested in the literature.

Experimental Section

We have used a CW mode locked Nd/YAG pumped dye laser (Coherent Nd/YAG Antares and Coherent 702 dye laser) as an excitation source. This source provides a high repetition rate (100 kHz–3.8 MHz) and short pulses (1 ps fwhm) at a wavelength of 580–620 nm. The frequency was doubled (to 290–310 nm) using a KDP-type I crystal. A repetition rate of 700 kHz was typically employed. Transient fluorescence was detected (without polarization selection) using time-correlated single photon counting (TCSPC), based on a monochromator (American Holographic DB-10), a Hamamatsu 1564U-01 photomultiplier, an S-20 photocathode, a Tennelec 854 TAC, and a Tennelec 454 discriminator. A personal computer was used as a multichannel analyzer (Nucleus Inc. PCA II), interfaced with an IBM personal computer for data storage and processing.

(16) Szabo, A. *J. Phys. Chem.* **1989**, *93*, 6929.
(17) Meot-Ner (Mautner), M. *J. Am. Chem. Soc.* **1986**, *108*, 6189.
(18) Popovych, O. *J. Phys. Chem.* **1984**, *88*, 4167.
(19) Marcus, Y. *Pure Appl. Chem.* **1990**, *62*, 899, Table 2.

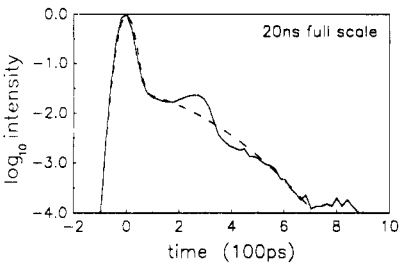

Figure 1. Instrument response function as obtained by measuring the reflected laser profile using the TCSPC system (full curve). The dashed curve is a fit to eq 1, with parameters in the text.

TABLE I: Technical Parameters in Fitting the Data of Figure 2

methanol vol fraction, %	TCSPC full scale, ns	background counts	$10^3 I_g$	α, ns^{-2}	shift, ps
0	20	10	1.1	690	0
17	20	14	1.0	740	7
29	20	7	1.6	780	−12
43	20	7	1.6	780	4
57	50	7	1.5	280	29
80	50	4	1.6	300	78

The overall instrument response function was determined by reflecting the 600-nm pulse from ground glass. The detected laser profile from a 20-ns full scale of the TCSPC system is shown in Figure 1. There is a sharp primary peak of about 55 ps fwhm, superimposed on a long tail, whose amplitude is about 3% that of the main peak. On a 50-ns scale (not shown) the width of the laser profile increases to about 70 ps fwhm. When the experimental data were fit, a somewhat larger width had to be used (see Table I).

8-Hydroxypyrene-1,3,6-trisulfonate (HPTS) was dissolved as its trisodium salt (Kodak, >99% chemically pure). Its concentration was 2×10^{-5} M. Deionized water had resistance >10 MΩ. Methanol was of spectroscopic grade by Merck. All chemicals were used without further purification. The solution pH was about 6. The laser pulse (≈300 nm) excites the HPTS to its second excited singlet state (S_2), which then relaxes via internal conversion to the first excited state (S_1). The transition dipole moment of S_2 was found to be approximately perpendicular to that of S_1. Thus, setting a polarizer at the magic angle of 54.7° to compensate for orientational relaxation cannot be used in this case.

The HPTS fluorescence spectrum consits of two bands. The blue band of the acidic (R*OH) form shifts from 441 nm in water to 424 nm in pure methanol. The green band of the basic (R^*O^-) form is almost solvent insensitive, shifting from 510 nm in water to 508 nm in methanol. We have monitored the R*OH fluorescence at 435 nm.

Results and Discussion

A. Technical. We have measured HPTS fluorescence following laser excitation in pure water and in five mixtures of varying water/methanol ratios using the TCSPC system (see Experimental Section) adjusted to a maximal count number of 100000–150000 counts/channel. For low methanol concentrations we have used a 20-ns full scale (1024 channels), while for high methanol content the full scale was adjusted to 50 ns. At the end of the scale the count rate was typically 10–20 counts/channel. The background prior to the laser pulse was steady at 0–2 counts/channel. We have nevertheless found it necessary to subtract a constant background of 5–15 counts/channel. The fact that this background is larger than in the dark could possibly be attributed to chemical impurities in the sample. We have also subtracted a signal due to R^*O^- fluorescence, which decays radiatively with a fluorescence lifetime $\tau_f = 5.3$ ns. This lifetime does not seem to vary with methanol concentration. The relative amplitude of the anion emission under the peak of the acidic, R*OH, form was estimated as 0.1%. This means that we have subtracted from the (normalized) blue signal a term of the form $I_g \exp(-t/\tau_f)$, with $I_g \approx 10^{-3}$. The exact background and I_g values subtracted are collected in Table I.

TABLE II: Physical Parameters as a Function of Methanol Fraction for the Data in Figure 2

vol %	wt %	mol %	ϵ	R_D, Å	D, Å²/ns	κ_d, ns⁻¹	κ_r, Å/ns	pK^*
0	0	0	80	28.3	930	8.0	7.2	1.28
17	14.0	8.4	78.5	28.8	710	4.3	6.7	1.55
28.6	24.0	15.1	75	30.2	570	3.0	5.9	1.74
43	37.2	25	69	32.8	450	1.5	4.2	2.05
57	51.1	37	63	35.9	370	0.8	3.2	2.40
80	76.0	64	49	46.2	260	0.22	0.62	2.89

It is more difficult to determine the radiative lifetime of the acidic form, which decays nonradiatively by proton transfer. To reduce the number of free parameters, we have assumed that the R*OH lifetime is equal to that of R^*O^-, namely, 5.3 ns, and invariant of methanol concentration. It is nevertheless possible that the "true" τ_f varies in the range 4–5 ns. To highlight the proton-transfer characteristics of the system, we routinely multiply the data by $\exp(t/\tau_f)$ to correct for the radiative decay.

Our theoretical calculation for the probability of observing a bound proton at time t, having started from the bound state at time $t = 0$, is denoted by $1 - S(t)$. Hence, $S(0) = 0$. The calculation is convoluted with the instrument response function (e.g., Figure 1) and compared with the corrected experimental data, normalized at $t = 0$ to the amplitude of the calculated curve. These corrected and normalized data are denoted by [R*OH] $\exp(t/\tau_f)$.

Convolution with the experimentally measured laser profile introduces noise into the calculation. We have therefore preferred to first fit the instrument response function by a smooth analytical formula. The fitting function for the measured laser intensity, $I_l(t)$, was chosen as

$$I_l(t) = \exp(-\alpha t^2) + AH(t)\exp[-\beta(t - t_0)^2] \qquad (1)$$

where $H(t)$ is the Heavyside function, $H(t) = 0$ if $t < 0$ and $H(t) = 1$ if $t \geq 0$. The fit for the 20-ns scale is shown in Figure 1. This function is normalized to an area of unity prior to convolution.

The values of the fitting parameters are $\alpha = 1000$ ns^{-2}, $A = 0.032$, $\beta = 8.6$ ns^{-2}, and $t_0 = -0.1$ ns. On the 50-ns scale, the fitting parameters were $\alpha = 530$ ns^{-2}, $A = 0.04$, $\beta = 7.5$ ns^{-2}, and $t_0 = -0.1$ ns. The main difference between the two scales is in the value of α, which corresponds to an increase of the main peak width from 53 to 72 ps fwhm. We have therefore decided to employ α as an adjustable parameter in fitting the experimental data and found that the best fit values of α are smaller by 10–30% than the above. In addition, the fit improves by shifting the relative position of the experimental and theoretical curves along the time axis, typically by less than one channel. These technical fitting parameters are also collected in Table I. The only reason for presenting them is to give the reader a feeling for the accuracy limits of the experimental setup.

B. The Diffusing Reversible Proton. Figure 2 shows our time-resolved data, measured at room temperature for several water–methanol mixtures and treated as described above. The data are shown on three scales: linear, semilogarithmic, and log–log. These were fitted, as in our earlier work,[10] subject to the assumption that the proton is diffusive and reacts reversibly with the excited-state anion. The fits are shown as dashed curves. Practically, we have solved the time-dependent Smoluchowski equation for the relative translational diffusion of the proton, subject to the Coulomb attraction force, the back-reaction boundary condition at the contact distance, and an initial bound state. The partial differential equation has been converted to a Master equation with detailed balancing, which was propagated in time using a Chebyshev expansion. Both theory and numerical procedures are described at length elsewhere.[10,14]

The theoretical fits involve several physical parameters, which are collected in Table II. The relative (translational) diffusion coefficient of the proton and HPTS anion was calculated as the sum of the individual diffusion coefficients. The proton diffusion coefficient, which is the dominant, was estimated from HCl conductivity data in methanol–water mixtures.[2] Due to the abnormal proton conductivity (Grotthuss mechanism), conductivity data give a better estimate for D than an extrapolation with viscosity.[7] The Coulomb attraction potential is $-R_D/r$, where the "Debye distance", R_D, is defined by $R_D \equiv |z_1 z_2| e^2/(k_B T \epsilon)$. e is the electronic charge. The ionic charge numbers, z_1 and z_2, were taken as $z_1 = 1$ and $z_2 = -4$ for H^+ and R^*O^-, respectively. $k_B T$ is the thermal energy, 2.48 kJ/mol at room temperature. ϵ is the (static) dielectric constant of the solvent, taken from recent time-domain reflectometry data.[20] These data are somewhat different from the values cited in ref 7, which were based on an empirical interpolation formula, and, in addition, produce a slightly higher value than customary for the static dielectric constant of water. The contact distance, a, was taken as 7 Å throughout. This roughly corresponds to the bare HPTS anion plus one or two solvation layers. The assumptions of a Coulomb interaction potential and diffusive motion are applied only to distances $r > a$. The kinetic parameters, which are the adjustable parameters of

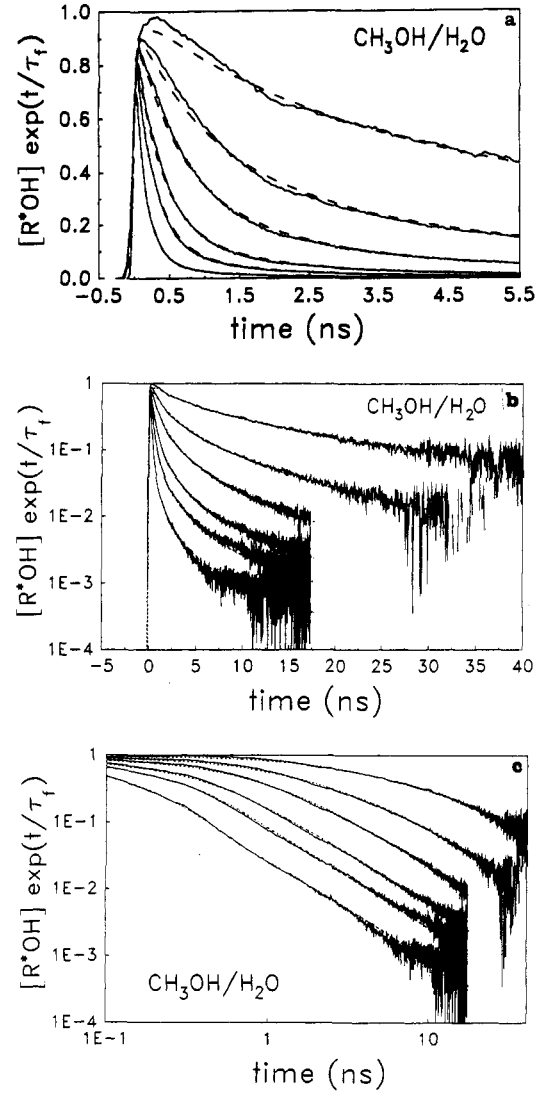

Figure 2. Fluorescence decay of excited HPTS in methanol–water solutions, corrected for background, anion fluorescence, and finite fluorescence lifetime (full curves). Dashed curves are theoretical fits to the reversible diffusion formalism with the parameters of Table II. Methanol fraction in solution is (bottom to top) 0, 17, 29, 43, 57, and 80% (by volume). (a) Linear scale; (b) semilogarithmic scale; (c) log–log scale. Each experimental curve was normalized to the peak of the corresponding calculated binding probability, $1 - S(t)$, which is unity at $t = 0$, after it was convoluted with an instrument response function whose area is unity. By this procedure we get an appropriate relative normalization of the decay curves in different solutions.

(20) Mashimo, S.; Kuwabara, S.; Yagihara, S.; Higasi, K. *J. Chem. Phys.* **1989**, *90*, 3292.

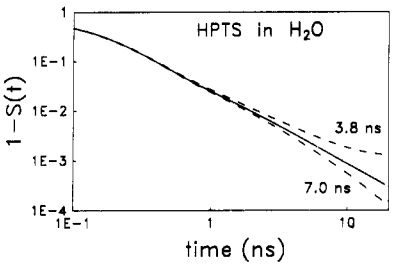

Figure 3. Effect of the estimated fluorescence lifetime on the observation of a power law decay. See text for discussion.

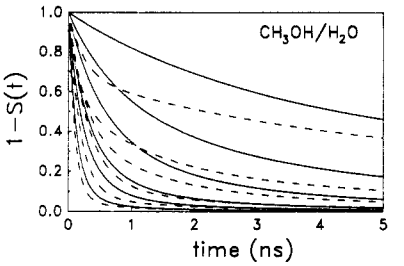

Figure 4. Comparison of the deconvoluted decay curves for the proton-bound state (full curves, parameters from Table II) with the multiexponential fit from Table I of ref 7 (dashed curves). Methanol fractions are as in Figure 2. See text for discussion.

the theory, are the dissociation and recombination rate parameters at contact. These are denoted, as before,[10] by κ_d and κ_r, respectively. κ_d determines the initial decay rate, while (mainly) R_D and κ_r determine the amplitude of the long-time tail.

The assumption that the anionic charge is constant as a function of composition may break down at high methanol concentrations, if the R^*O^- anion is associated with Na^+ counterions. To check for ionic association, we have repeated the kinetic measurements for varying HPTS concentrations in the range 10^{-7}–10^{-3} M. For the 80% (v) methanol solution, we find no change in the decay profile. However, for a 90% (v) methanol solution we notice an already marked dependence on HPTS concentration, with a diminished long-time tail for the higher HPTS concentrations. We tentatively conclude that for the methanol content used in the present study, up to 80% (v), ionic association is negligible.

Returning to Figure 2, our first observation is that there is an excellent overall agreement between experiment and theory in all solutions studied. Already at moderately long times the data tend to a power law. This is seen most clearly on the log–log scale, where the data approach straight parallel lines of slope $^3/_2$. The largest range for the power law behavior is at low methanol concentrations. This is because at large methanol content the reaction proceeds so slowly that the signal decays radiatively before the asymptotic limit is reached. In water and the 17% methanol (v) solutions, the asymptotic behavior actually begins around 0.5 ns, earlier than what seems from Figure 2. This is due to the tail and secondary peak (at ~300 ps) in the laser profile (see Figure 1). It results in the small hump which is most conspicuous on the log–log scale around 300–800 ps (Figure 2c).

The Dhahran group[7] has raised the possibility that the power law decay is an artifact due to inaccurate estimates of τ_f. To test this, we plot in Figure 3 the calculated decay curve in water on a log–log scale (full line). This represents the deconvoluted data, corrected for a "correct" radiative lifetime, $\tau_f = 5.3$ ns. The two dashed lines represent the deconvoluted data, corrected for two extreme "incorrect" but plausible values of the radiative lifetime, $\tau_f' = 3.8$ and 7.0 ns. In other words, the dashed curves are obtained by multiplying the full curve by $\exp(t/\tau_f' - t/\tau_f)$. As can be seen, the dashed curves bracket rather closely the asymptotic straight line. Hence, uncertainties in τ_f cannot completely obscure the long-time power law decay.

Magnification of the data on a linear scale (Figure 2a) reveals some short-time disagreements between experiment and theory. These deviations involve, in fact, a slow rise time in the R*OH signal, which we attribute to rotational diffusion. Rotational diffusion times increase with methanol content due to increase in solvent viscosity from, say, 150 ps in pure water to 250–300 ps in an 80% (v) methanol mixture. Careful monitoring of both polarization components will be required to fully account for this effect. This is difficult in the present setup, where absorption and emission involve two different electronic states (see Experimental Section). It is nevertheless clear from the data that no fast short-time decay component is detectable.

The question then arises as to why did the Dhahran group conclude that the data show a fast initial decay. To check this, we compare in Figure 4 our deconvoluted data (full curves) with the deconvoluted data represented as the multiexponential fit parameters in Table I of ref 7 (dashed curves). We have applied linear interpolation to these parameters to adjust to methanol volume fractions used in the present study[21] and multiplied by $\exp(t/\tau_f)$. The deconvoluted Dhahran data do show a fast decay phase at high methanol concentrations. Indeed, the data in Table I of ref 7 include a fast component (τ_3) possessing a considerable amplitude (A_3) even at high methanol concentrations. In contrast, the raw data in Figure 7 of ref 7 do not seem to show such a behavior. These raw data resemble our data, which show no decay component faster than $1/\kappa_d$ (see Table II). We therefore suspect an error in the deconvolution routine used by the Dhahran group.[7] As far as can be concluded by a careful examination of the transient HPTS fluorescence decay data in water–methanol mixtures, there is no evidence for a water diffusion mechanism,[7] nor is there evidence for a significant deviation from the reversible proton diffusion mechanism.[10]

C. Composition Dependence of the Equilibrium Coefficient. Our direct determination of both dissociation and recombination rate parameters (Table II) provides a unique example where the excited-state rate and equilibrium coefficients are determined by a single transient measurement. Using the rate parameters, it is a simple matter to evaluate the equilibrium (dissociation) coefficient, K, from[10]

$$K^{-1} = [4\pi a^2 N_A \kappa_r \exp(R_D/a)]/10^{27}\kappa_d \qquad (2)$$

In eq 2, N_A is Avogadro's number and the factor $10^{-27}N_A$ converts the concentration units from molecules/Å^3 to molar. The excited HPTS pK values, $pK \equiv -\log_{10} K$, are also collected in Table II. To adhere with conventions in the literature, a notation pK^* is used for excited-state pK (although an asterisk is usually not employed in designating excited-state rate coefficients).

A question may arise whether equilibrium data obtained from such fast kinetic measurements reflect true thermodynamic equilibrium, in which the solvent has achieved its relaxed configuration around the excited molecule. It is customary to assume[22] that the dielectric relaxation time (which increases from about 9 ps in water to 60 ps in methanol[20]) is an upper bound to solvent relaxation times. Recent "transient solvation" measurements[23] indeed show that solvent relaxation in both water and methanol is nonexponential in time, the slower component being about 1 ps for water and 10 ps for methanol. Since proton dissociation also slows down considerably upon addition of methanol, we conclude that solvation times are approximately 2 orders of magnitude faster than proton transfer in all mixtures studied.

Figure 5 compares our $\Delta pK \equiv pK_{mixture} - pK_{water}$ values with those of ground-state phenol derivatives.[24] Our first observation is that the points generally fall on the same curve. Older ΔpK^* data[25] for excited 2-naphthol (not shown) also fall on the same

(21) For two concentrations the pre-exponential factors in Table I of ref 7 do not add up to unity. We have therefore taken the liberty to change A_1 for 70% methanol (v) from 0.399 to 0.288 and A_2 for 20% methanol (v) from 0.022 to 0.107. Another typographical error occurred in the right column of Table II in ref 7, where for $t = 0.15$ ns the multiexponential decay gives 0.250 instead of 0.263.

(22) Kosower, E. M.; Huppert, D. *Annu. Rev. Phys. Chem.* **1986**, *37*, 127.
(23) Jarzeba, W.; Walker, G. C.; Johnson, A. E.; Barbara, P. F. *Chem. Phys.* **1991**, *152*, 57.
(24) Parsons, G. H.; Rochester, C. H. *J. Chem. Soc., Faraday Trans. 1* **1975**, *71*, 1058.

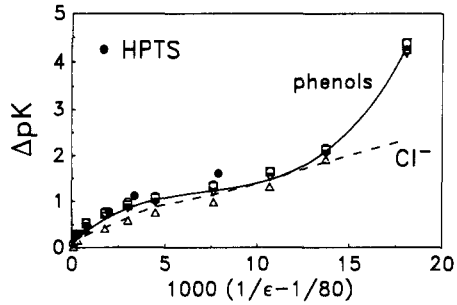

Figure 5. Comparison of the (methanol–water) composition dependence of protonation equilibrium coefficients for excited HPTS (closed circles, Table II) and ground-state phenols[24] (open symbols): (○) phenol; (□) *p*-methylphenol; (▽) *p*-bromophenol; (△) *p*-nitrophenol. The full curve is the best third-order polynomial fit to the average of the four phenol data sets. The dashed curve is the best fit to the standard transfer free energy of chloride,[19] divided by $2.3RT$ = 5.7 kJ/mol.

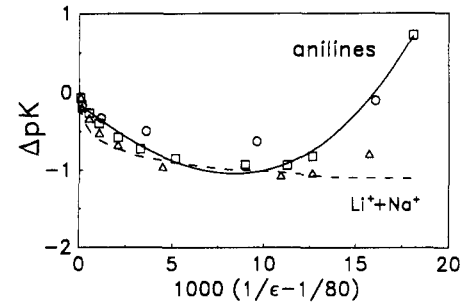

Figure 6. Composition dependence of the equilibrium coefficients for the protonation of anilines:[26] (○) aniline; (□) *o*-chloroaniline; (△) *m*-nitroaniline. The full curve is the best third-order polynomial fit to the *o*-chloroaniline data. The dashed curve is the average standard free energy of transfer of lithium and sodium cations,[19] divided by $-2.3RT$.

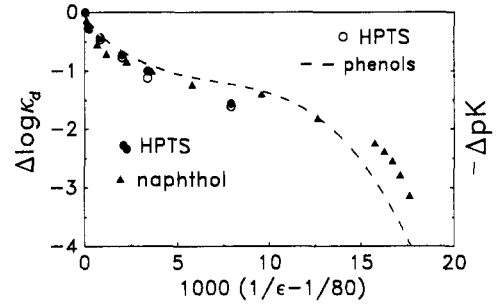

Figure 7. Comparison of standard free energy of transfer of protons from water to aqueous methanolic solutions, obtained as the difference of the bold and dashed curves in Figures 5 and 6, with the "best" selection of literature values[19] (full circles with interpolating curve).

"universal" curve. The fact that HPTS, whose pK^* in water is about 1.3, and various phenols, with p$K_{water} \approx 7$–10, show the same composition dependence indicates that differential solvation of the ROH acid is negligible. Otherwise, one may expect that stronger acids with a more polar OH bond will show a larger sensitivity to solvent dielectric properties. Hence, the major contribution is from differences in solvation of RO^-. Additionally, phenols and pyrenes vary in both size and total charge change, which for HPTS is −3 to −4, while for phenols it is 0 to −1. A simple Born solvation model for the whole anion[26] will predict different slopes for HPTS and phenols. Figure 5 is best interpreted in terms of localized solvation of the oxide ion. The sulfonate groups are presumably solvated independently from each other and from the protonation site. Their contribution to the protonation free energy change therefore vanishes. The only contributer is the oxide ion with its specific solvation. This agrees with the observation by Taft[27] that pK values of phenols are 6–7 times less sensitive to ring substituents in solution as compared to in the gas phase. Indeed, if the negative charge is delocalized by the solvent, the importance of substituents in achieving the same goal diminishes.[27]

A quantitative understanding of the pK variations may be obtained by modeling the localized oxide anion by a reference anion of a similar size, for example, chloride (data for fluoride are scarce[19]). The dashed curve in Figure 5 is $\Delta G_t(Cl^-)/2.3RT$, where $\Delta G_t(Cl^-)$ is the standard free energy of transfer of a chloride anion from water to the appropriate aqueous methanol mixture, $\Delta G_t(Cl^-) \equiv G_{mixture}(Cl^-) - G_{water}(Cl^-)$. We use the best polynomial fit to averaged values of many experimental compilations summarized in ref 19. The chloride data fits the Born solvation model,[26] in which $\Delta pK = 123(1/\epsilon - 1/80)r_A^{-1}$, with 80 being (approximately) the dielectric constant of pure water at room temperature[20] and an anionic radius, r_A, which is very nearly 1 Å. The only deviation from this behavior occurs near pure water.

The most conspicuous difference between the ΔpK data and the chloride solvation free energy is that the latter is linear in $1/\epsilon$ near pure methanol while the ΔpK data show a sharp rise near pure methanol. This difference should be ascribed to proton solvation. To eliminate specific substituent effects, we average the phenol data and fit them to a third-order polynomial, ΔpK(phenols) = $0.098 + 3.59y - 4.27y^2 + 1.97y^3$, where $y \equiv 100(1/\epsilon - 1/80)$. This fit (which is a purely technical device for data smoothing purposes) is shown by the bold curve in Figure 5. The difference between the bold and dashed curves is therefore our best estimate for the standard free energy of transfer of a proton from water to aqueous methanolic solutions, namely, $\Delta G_t(H^+) = 2.3RT\Delta pK(\text{phenols}) - \Delta G_t(Cl^-)$. The quantitative success of this procedure will be demonstrated below.

As a further test for this simple analysis, let us consider the variation in the ΔpK of protonated anilines (anilinium ions).[26] Here the charge change is from +1 to 0, so a reduction of ϵ destabilizes the reactants and increases the acidity. Above 80% (w) methanol, the solvated proton becomes less stable, with the resulting minimum in the plot of ΔpK against $1/\epsilon$ shown in Figure 6. The typical behavior exemplified by *o*-chloroanilinium is fitted to a third-order polynomial, ΔpK(anilines) = $-0.142 - 1.92y + 0.75y^2 + 0.317y^3$, shown as the bold curve in Figure 6. Assuming, again, that solvation is localized to the ammonium moiety, we choose as a reference cation the average of lithium and sodium. The averaging wil tend to cancel specific size effects. The dashed curve shows $-{}^1/_2[\Delta G_t(Li^+) + \Delta G_t(Na^+)]/2.3RT$, using the selected values of ref 19. This "typical cation" deviates from the Born approximation more than our "typical anion" (Figure 5), as can be seen from the fact that the dashed curve in Figure 6 is not linear. The difference between the full and dashed curves is again expected to describe proton solvation.

The success of the above subtraction procedure is demonstrated in Figure 7, which shows the standard free energy of transfer of a proton from water to methanol–water mixtures. The selected literature values, taken from ref 19, are shown as the full circles connected by the full curve. The open symbols show $\Delta G_t(H^+)$ as estimated from the measured ΔpK values of phenols and anilines by the procedure described above. The agreement is remarkable, since even the shallow maximum and minimum in $\Delta G_t(H^+)$ are reproduced. This is due to our repeated averaging strategy, in which specific effects will tend to cancel out. The "selected" values in ref 19 were picked as the average of 4 of 15 experimental compilations which, with the exception of the selected 4, vary widely in their $\Delta G_t(H^+)$ values. The agreement shown in Figure 7 lends further support to the selection in ref 19.

We have thus obtained a quantitative analysis of pK variations in methanol–water mixtures. According to this analysis, up to 80% (w) methanol, counterion destabilization is dominant, whereas at higher methanol content proton destabilization becomes important. Furthermore, solvation of the counterion is localized and can be mimicked by a suitable reference ion.

It follows from Figure 7 that proton solvation is nonclassical and deviates significantly from the Born model. Up to 80% (w)

(25) Trieff, N. M.; Sundheim, B. R. *J. Chem. Phys.* **1965**, *69*, 2044.
(26) Bates, R. G.; Robinson, R. A. In *Chemical Physics of Ionic Solutions*; Conway, B. E., Barradas, R. G., Eds.; Wiley: New York, 1966; Chapter 12, p 211.
(27) Taft, R. W. *Prog. Phys. Org. Chem.* **1983**, *14*, 247.

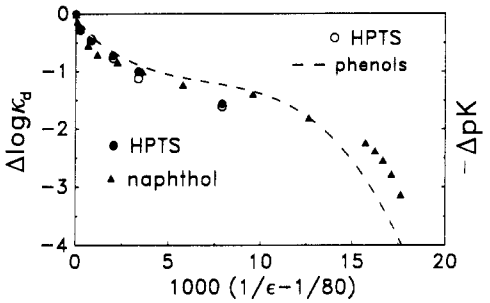

Figure 8. Comparison of the deprotonation rates of excited pyranine (full circles, Table II) and excited 1-naphthol (full triangles, Table III) with pK values of excited pyranine (open circles, Table II), and "average" ground-state phenol (dashed curve, Figure 5).

TABLE III: Proton Dissociation Rate Coefficients for Excited 1-Naphthol (S_1)

wt %	τ_{obs}, ns	κ_d, ns^{-1}	wt %	τ_{obs}, ns	κ_d, ns^{-1}
0	0.040	24.8	76.0	0.84	1.00
7.68	0.055	18.0	87.7	1.75	0.380
13.7	0.067	14.7	93.8	3.0	0.141
28.3	0.140	6.97	95.0	3.4	0.102
34.5	0.20	4.82	96.2	3.8	0.071
44.2	0.27	3.53	97.5	4.3	0.040
54.3	0.38	2.44	98.7	4.75	0.018
64.9	0.61	1.45			

methanol, there are only minor variations in $\Delta G_t(H^+)$, while sharp destabilization is evident near pure methanol. This has been qualitatively interpreted by Bates and Robinson[26] as evidence that the proton resides on a water molecule. The H_3O^+ is further solvated by three ligands, which can be either water or methanol molecules, their different combinations resulting in minor free energy differences. Only when the last, central water molecule is replaced by methanol does one observe a substantial increase in ΔG. This interpretation is substantiated by recent experimental work.[28]

D. Composition Dependence of the Rate Coefficients. The dependence of the dissociation parameter, κ_d, on the mixture's dielectric constant is shown in Figure 8. As previously reported,[3] κ_d decreases monotonically with increasing methanol content.[29] Since it is impossible to monitor proton dissociation from HPTS above 80% (w) methanol, we have also measured proton dissociation rates from excited 1-naphthol (Table III). Dissociation of 1-naphthol in water is about 3 times faster than that of HPTS, and geminate recombination is negligible. Its nearly exponential fluorescence decay, $\exp(-t/\tau_{obs})$, enables the evaluation of κ_d from $\kappa_d = 1/\tau_{obs} - 1/\tau_f$, with $\tau_f \approx 5.2$ ns. This procedure allows the determination of κ_d up to 90% (w) methanol, thus extending previous experiments[5] to the methanol-rich region. Above 90% (w), the quoted values (Table III) should be considered rough estimates.

Although HPTS and naphthol have different charges and molecular sizes, the dissociation parameters fall approximately on the same curve (Figure 8). The variation with solvent composition is qualitatively similar to that of ΔpK values of phenols (Figure 5). For HPTS, where both forward and reverse rate parameters are determinable, we may compare directly variations in κ_d (full circles) and in K (open circles). It is clear from the figure that in this range

$$\Delta \log \kappa_d \approx -\Delta pK \qquad (3)$$

This means that $\kappa_r \exp(R_D/a)$ is approximately independent of composition (see eq 2), which can be verified directly from the data in Table II. Relation 3 implies that HPTS data for methanol–water mixtures fall on the straight Bronsted plot observed for numerous other proton dissociation reactions (e.g., Figure 4 in ref 30). In terms of more extended structure–reactivity correlations,[31] one may conclude that (i) proton transfer to solvent involves a very small intrinsic barrier and (ii) dissociation reactions studied so far are in the endothermic regime.

We are now in a position to summarize the trends in reaction rate coefficients for proton dissociation from hydroxyaryls to methanol–water mixtures. In the composition range of approximatly 0–80% (w) methanol, the dissociation rate decreases due to decreased thermodynamic stability (increasing $\Delta G°$) of the product anion, while proton stability hardly changes. For an opposite charge arrangement, such as the dissociation of charged anilines, one would expect to see an *increase* in the rate coefficient in this regime. This is verified in kinetic measurements of proton dissociation from excited protonated aminopyrenes.[28] The latter observation contrasts with models[3-6] ascribing the variation in κ_d solely to dilution of large "water clusters", since such models predict that proton dissociation rates should always decrease with increasing methanolic content, irrespective of the charge on the proton donor.

In the range 80–100% (w) methanol, a drastic decrease of about 2 decades is expected for all acids due to destabilization of the solvated proton as it spends more time on methanol centers with the decreasing availability of water molecules. Accurate determination of deprotonation rates by transient fluorescence methods is restricted in this region by finite radiative lifetimes. We have therefore investigated proton transfer to solvent from one of the fastest excited donors available, 1-naphthol (Table III). Our data, shown in Figure 8 (triangles), indeed exhibit a sharp decrease in the methanol-rich region which apparently parallels the sharp increase in proton free energy of transfer of Figure 7. Since, in our view, earlier measurements[3-5] in the water-rich region reflect primarily the effect of counterion solvation, these data represent a first real kinetic evidence for the effect of proton solvation on the process of proton dissociation from excited hydroxyaryls.

Conclusion

We have measured proton-transfer dynamics from an excited dye molecule to methanol–water mixtures by monitoring the transient fluorescence signal. Using a fast laser as the excitation source and single photon counting for fluorescence detection, we were able to obtain the fluorescence decay curves over more than 4 orders of magnitude in intensity with good signal to noise ratio. Our data, in all mixtures studied, show an initial exponential decay turning over to a power law ($t^{-3/2}$) at long times. This behavior fits quantitatively with our interpretation of a reversible diffusing proton,[10] as demonstrated from the solution of a time-dependent Smoluchowski equation for a Coulomb potential and with a back-reaction boundary condition.

In the water-rich region, we find no evidence for a suggested mechanism,[7] according to which the rate-limiting step is diffusion of a water molecule to the excited anion to form a bimolecular reactive encounter. Such a mechanism should have resulted in a fast nonexponential initial transient rather than a long-time power law decay. We see no evidence of a fast transient, while the long-time tail is clearly observed. Examination of the data in ref 7 suggests that the water diffusion mechanism may have been motivated by a faulty deconvolution procedure.

In addition to the failure to detect any evidence for water diffusion in the transient kinetic data, we have shown that there is no thermodynamic requirement for water diffusion because in the water-rich region, where proton dissociation from excited hydroxyaryls can be monitored, the decrease in the dissociation rate coefficient reflects almost entirely the destabilization of the anion. The kinetic model,[4-6] which postulated availability of large water clusters as the only factor governing the rate of proton transfer to solvent, is therefore at odds with existing thermodynamic data as well as with the kinetic data collected in the present work.

Our ability to determine both forward and reverse rate coefficients, and hence also the equilibrium coefficient, for the same system using a single transient measurement enabled us to prove

(28) Pines, E.; Fleming, G. R. *J. Phys. Chem.* **1991**, this issue.
(29) This contrasts with the behavior of k_1 in Table III of ref 7, which does not decrease monotonically with increasing methanol weight fraction.
(30) Gutman, M.; Nachliel, E. *Biochim. Biophys. Acta* **1990**, *1015*, 391.
(31) Agmon, N. *Int. J. Chem. Kinet.* **1981**, *13*, 333.

directly that solvent variations in the dissociation rate coefficient are equal to variations in the (dissociation) equilibrium coefficient. Comparing the composition dependence of the equilibrium coefficient for pyranine with that of various phenols, we found nearly identical solvent-induced pK variations, which we therefore attribute to localized solvation at the oxide ion. The localized solvation site could be modeled as a small anion (chloride), which accounted for most of the observed free energy variation in the water-rich region. Deviations, mostly in the methanol-rich region, are attributed to proton solvation and indeed yield a beautiful quantitative agreement with literature compilations of proton free energy of transfer data. Using the fast proton donor 1-naphthol, we obtained a first kinetic evidence for the sharp increase in $\Delta G_t(H^+)$ near pure methanol.

The proton solvation data are highly nonclassical in their deviation from the Born solvation model. Interpreted in terms of the stability of hydrogen-bonded clusters, one would conclude that in water-methanol mixtures the stability of all clusters is nearly identical provided that they are centered around a protonated water core. Only when this core is replaced by protonated methanol does the cluster stability diminish. Statistical mechanics of proton solvation may further clarify these issues in the future.

Acknowledgment. We are grateful to Profs. C. Lifshitz, Y. Marcus, and G. W. Robinson for helpful discussions and comments on the manuscript. Work was supported in part by Grants 86-00197 and 88-00125 from the U.S.-Israel Binational Science Foundation (BSF), Jerusalem, Israel, and by a grant from the James Franck Binational German-Israeli Program in Laser-Matter Interaction. The Fritz Haber Research Center is supported by the Minerva Gesellschaft für die Forschung, München, BRD.

Registry No. HPTS, 6358-69-6; 1-naphthol, 90-15-3.

Time-Dependent Calculation of Thermally Averaged Reaction Rate Constants: Dynamical Displacement Operator Treatment

Nancy Makri[†]

Department of Chemistry, Harvard University, 12 Oxford Street, Cambridge, Massachusetts 02138
(Received: April 4, 1991)

The time-dependent operator formulation of the reactive flux-side correlation function [*J. Chem. Phys.* **1991**, *94*, 4949], whose long-time limit yields the quantum mechanical Boltzmann-averaged rate constant, is optimized by including displacement operators in the expansion of the complex time evolution operator. The advantage of this new treatment is that very few terms are needed for the representation of the propagator, thus significantly reducing the numerical effort required in the calculation.

I. Introduction

Recently, we presented[1] a fully quantum mechanical methodology for calculating finite temperature reaction rate constants. This formulation can be used to study the reaction kinetics of polyatomic systems, provided that the Hamiltonian can be approximately decomposed into a system coupled (strongly) to a bath. Reaction path models[2-5] are known to achieve such a decomposition, and thus the above rate formalism can be applied to reactive molecular collisions. In addition to gas-phase chemistry, this approach is expected to be relevant and useful also in the field of gas-solid interactions; for example, it can be used to study the role of lattice vibrations (phonons) in determining the rates of dissociation and of diffusion of light species, such as hydrogen or deuterium, on surfaces. Application of these ideas to the dynamics of quantum particles (e.g., electrons) in fluids may be possible but is less straightforward.

The calculation is based on the evaluation of a flux correlation function obtained by Miller et al.[6-8] The multidimensional quantum time evolution operator is represented by a mean field form in the space of the bath degrees of freedom, but is constructed to incorporate correlation between the system (i.e., the reaction coordinate) and the bath. This ansatz for the propagator is the operator analogue of the time-dependent self-consistent-field approximation with explicit two-body correlations proposed earlier[9] and leads to *linear* increase in numerical effort with the number of bath degrees of freedom, without significant loss of accuracy. The Boltzmann average is performed by using a mixed coordinate/operator representation of the density matrix,[10,11] which allows the canonical rate constant to be evaluated *directly* from the solution of a set of temperature-dependent coupled first order differential equations in time with well-behaved initial conditions.

In this paper we present a modified scheme for expanding the complex time evolution operator (i.e., the density matrix) that leads to accelerated convergence with respect to the number of required bath excitation operators. Specifically, we incorporate the system-bath coupling in the zeroth-order term of the expansion via proper displacement operators. This treatment causes the strongest correlation effects to be described by very few terms that correspond to low-order excitation of the bath.

[†] Harvard Junior Fellow. Present address: School of Chemical Sciences, University of Illinois, Urbana, IL 61801.

(1) Makri, N. *J. Chem. Phys.* **1991**, *94*, 4949.
(2) Marcus, R. A. *J. Chem. Phys.* **1964**, *41*, 610; **1966**, *45*, 4493, 4500; **1968**, *49*, 2610.
(3) Hofacker, G. L. *Z. Naturforsch. A* **1963**, *18*, 607. Fischer, S. F.; Hofacker, G. L.; Seiler, R. *J. Chem. Phys.* **1969**, *51*, 3951.
(4) (a) Miller, W. H.; Handy, N. C.; Adams, J. E. *J. Chem. Phys.* **1980**, *72*, 99. Miller, W. H. In *Potential Energy Surfaces and Dynamics Calculations*; Truhlar, D. G., Ed.; Plenum: New York, 1981. Miller, W. H. *J. Chem. Phys.* **1983**, *87*, 3811. Carrington, Jr., T.; Miller, H. *J. Chem. Phys.* **1984**, *81*, 3942. Miller, W. H. In *The Theory of Chemical Reaction Dynamics*; Clary, D. C., Ed.; Reidel: Boston, 1986. (b) Miller, W. H.; Ruf, B. A.; Chang, Y. T. *J. Chem. Phys.* **1988**, *89*, 6298. (c) Ruf, B. A.; Miller, W. H. *J. Chem. Soc., Faraday Trans. 2* **1988**, 84.
(5) Truhlar, D. G.; Brown, F. B.; Steckler, R.; Isaacson, A. D. In *The Theory of Chemical Reaction Dynamics*; Clary, D. C., Reidel: Boston, 1986. Duff, J. W.; Truhlar, D. G. *J. Chem. Phys.* **1975**, *62*, 2477.
(6) (a) Miller, W. H. *J. Chem. Phys.* **1974**, *61*, 1823; *Acc. Chem. Res.* **1976**, *9*, 306.
(7) Miller, W. H.; Schwartz, S. D.; Tromp, J. W. *J. Chem. Phys.* **1983**, *79*, 4889.
(8) For a survey of other methods for calculating flux correlation functions see ref 1.
(9) Makri, N. *Chem. Phys. Lett.* **1990**, *169*, 541.
(10) Abrikosov, A. A.; Gorkov, L. P.; Dzyaloshinski, I. E. *Methods of Quantum Field Theory in Statistical Physics*; Dover: New York, 1975.
(11) (a) Stiles, M. D.; Wilkins, J. W.; Persson, M. *Phys. Rev. B* **1966**, *34*, 4490. (b) Jackson, B. *J. Chem. Phys.* **1986**, *84*, 3535; **1988**, *88*, 1383; **1988**, *89*, 2473.

0022-3654/91/2095-10413$02.50/0